THE EFFECT OF THE SHAPE OF SANDS ON THE PORE PRESSURE IN THE SEABED AND SEDIMENT TRANSPORT

Sep. 5th, 2005, APAC Jeju, Korea

Daisuke TATSUMI (PARI, JAPAN)

Shinji SATO (UT, JAPAN)

$\eta(t) \approx p(t)$

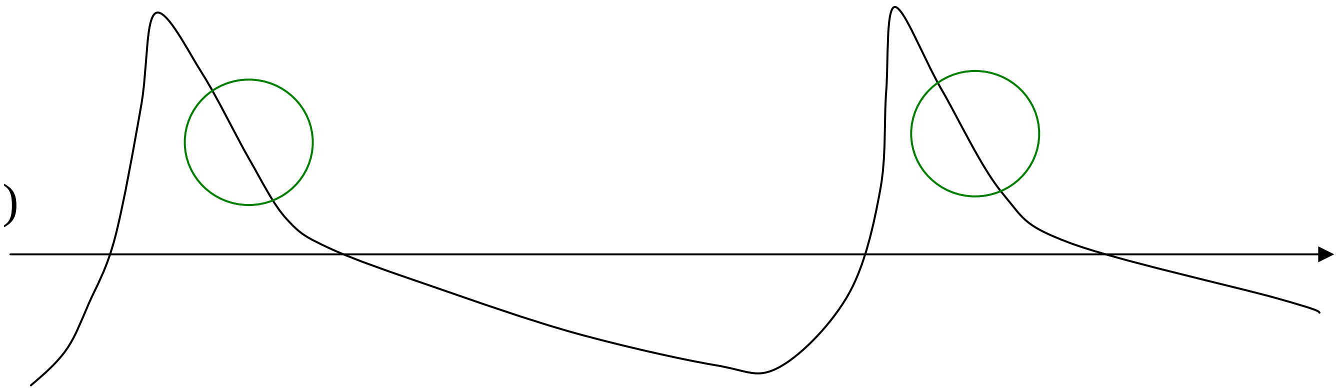

sudden decrease in water pressure

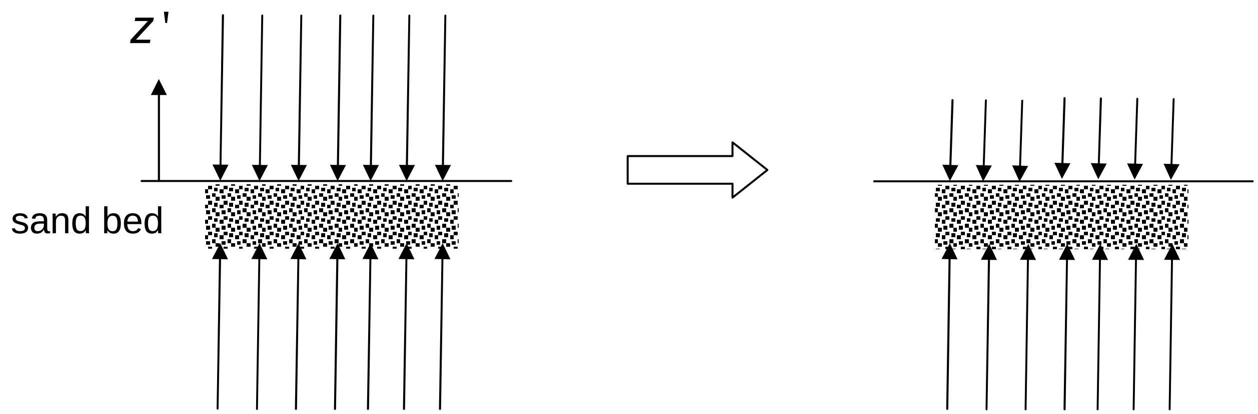

$$\frac{\partial p}{\partial z'}\Big|_{z'=0} < 0$$

mobilize?

slow decrease in <u>pore water pressure</u>

porosity, shape of particles
saturation ratio, …

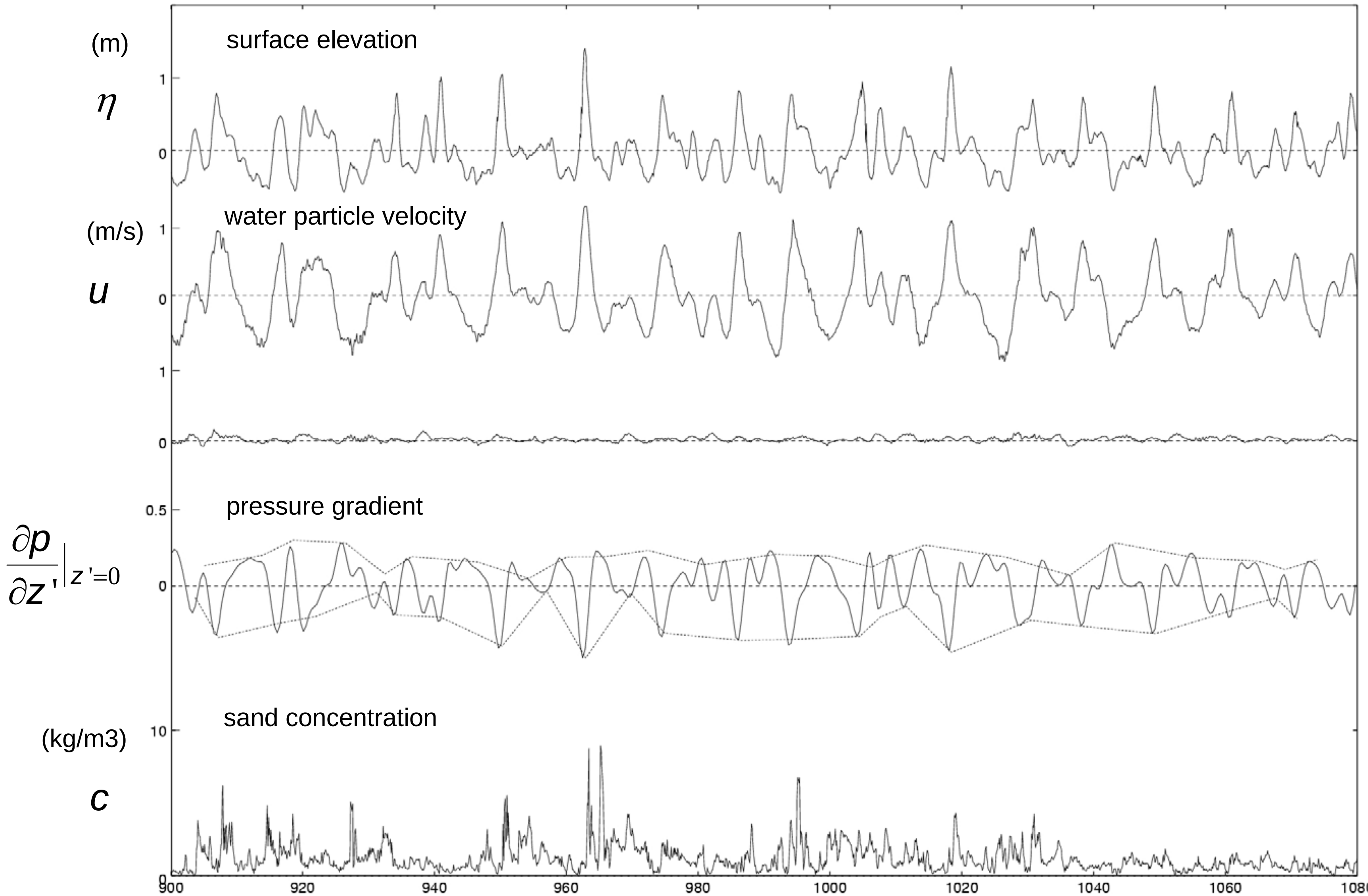

3 minute record of suspended sand concentration, Ajigaura, moderate waves

→ No evidence found for pore pressure sensitivity

2-1. Sediment Properties

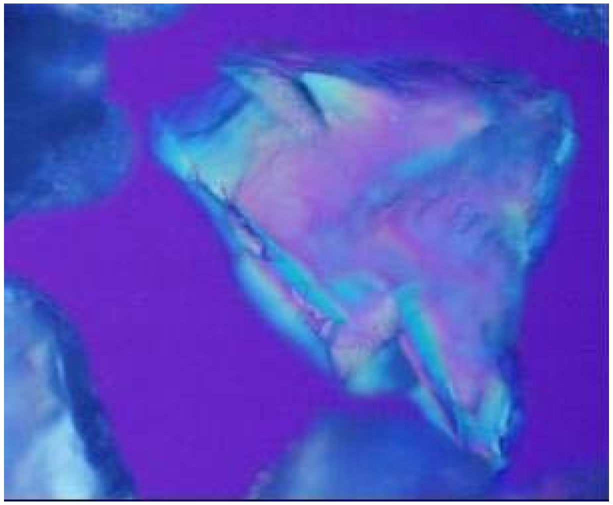

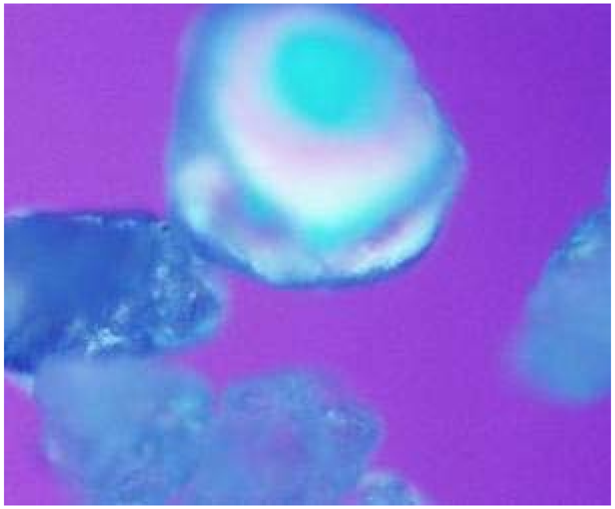

Above: Angular
Below: Round

Same size and density for angular and round sands

	Angular	Round
Median diameter (mm)	0.25	0.23
Sorting coefficient	1.208	1.212
Density (g/cm3)	2.644	2.644
Settling velocity (cm/s)	3.24	2.76
Angle of repose (degree)	33.3	30.3
Cmax (Maximum sediment concentration)	0.550	0.611
Saturation ratio	0.977	0.987
Coefficient of consolidation (m2/s)	1.699	2.364

Angular sand : larger frictional resistance, larger porosity, harder to be consolidated

Flume experiments

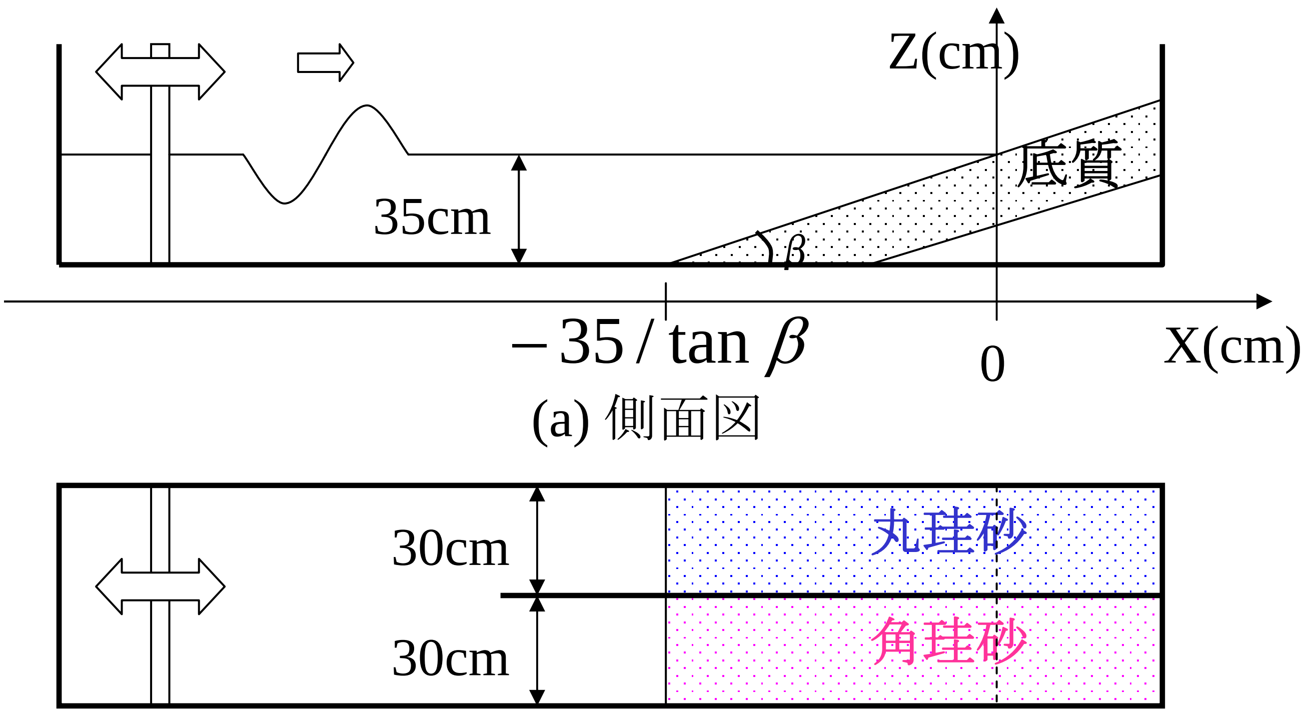

(a) 側面図

(b) 平面図

()

(a) 堆積型(Case12)

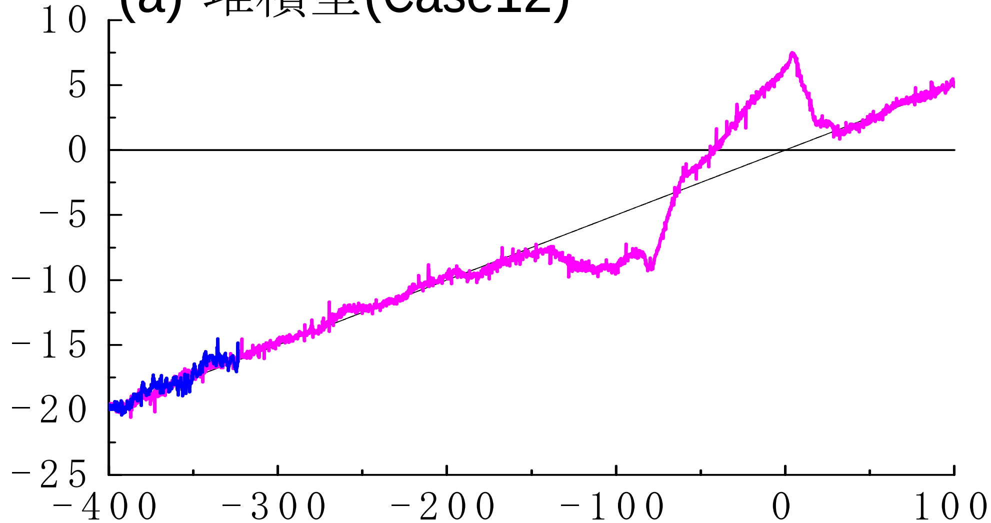

(b) 侵食型(Case14)

()

2-2. Method of Laboratory Experiments (1)

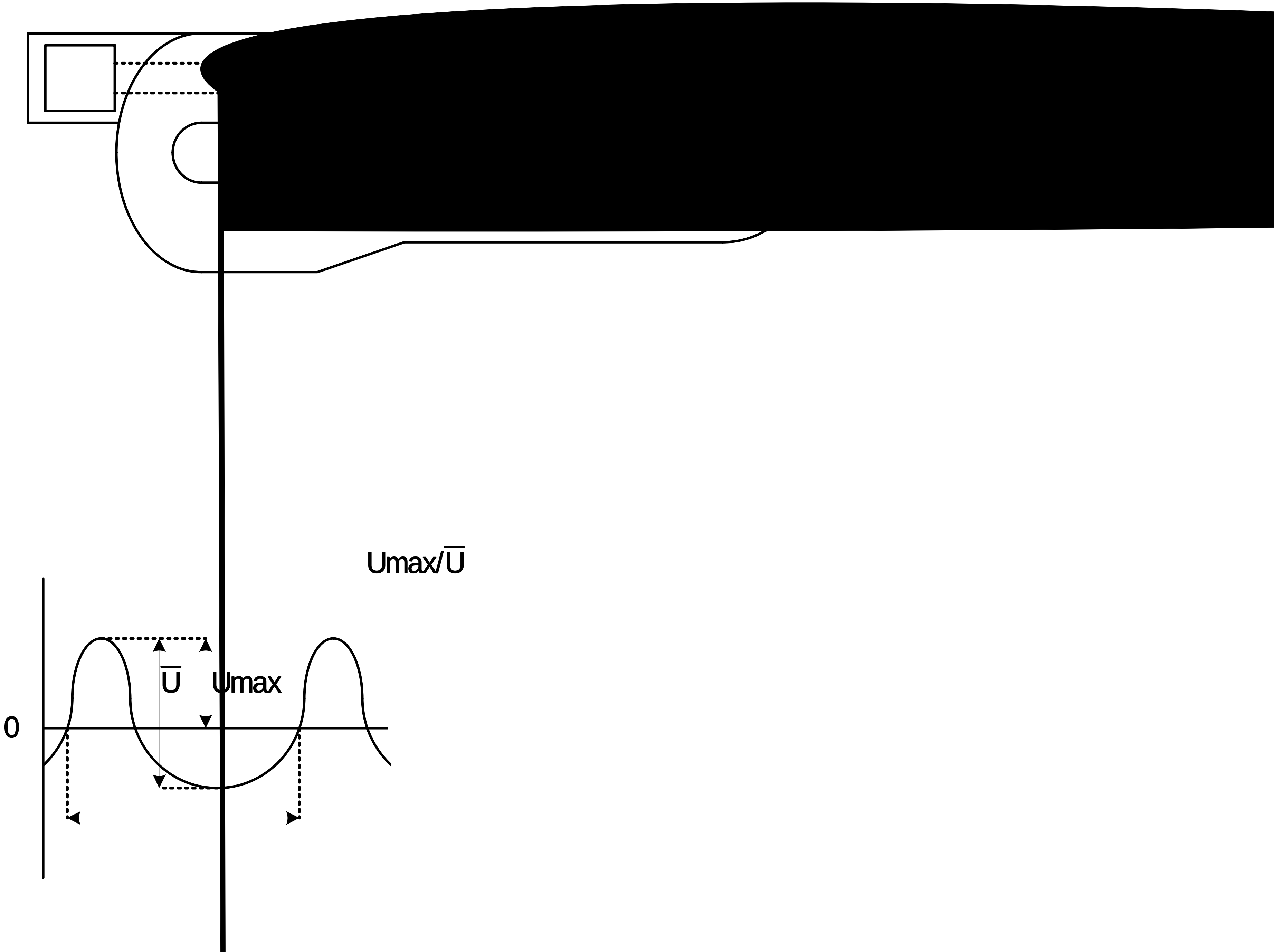

2-3. Method of Laboratory Experiments (2)

Measured items

1. **Sediment transport rate by comparing the weight of sand before and after experiments**
2. **Suspended sediment concentration by the brightness of video images**
3. **Horizontal velocity by PIV technique**

Sand flux per unit width can be calculated

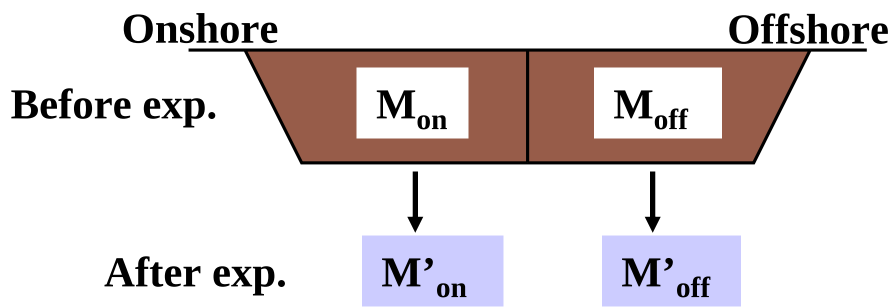

Sediment transport rate: $(M'_{on}-M_{on})-(M'_{off}-M_{off})$

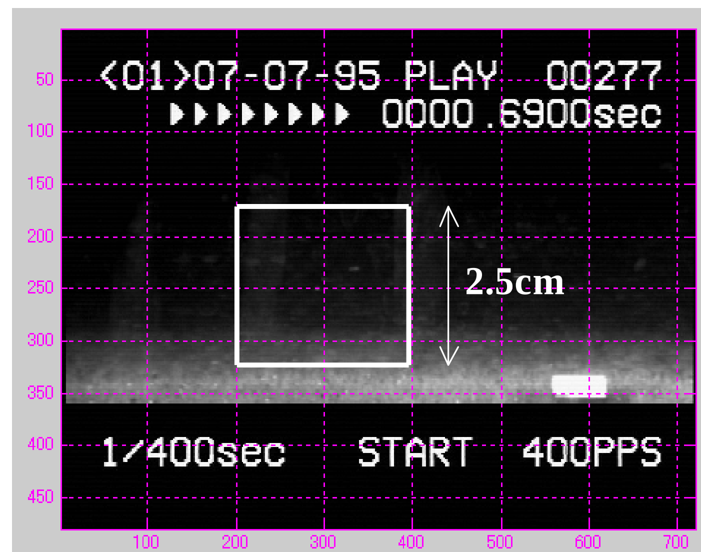

Image resolution: 1 pixel = 0.0178(cm), dt = 1/400(s)

2-4. Experimental Results (1)

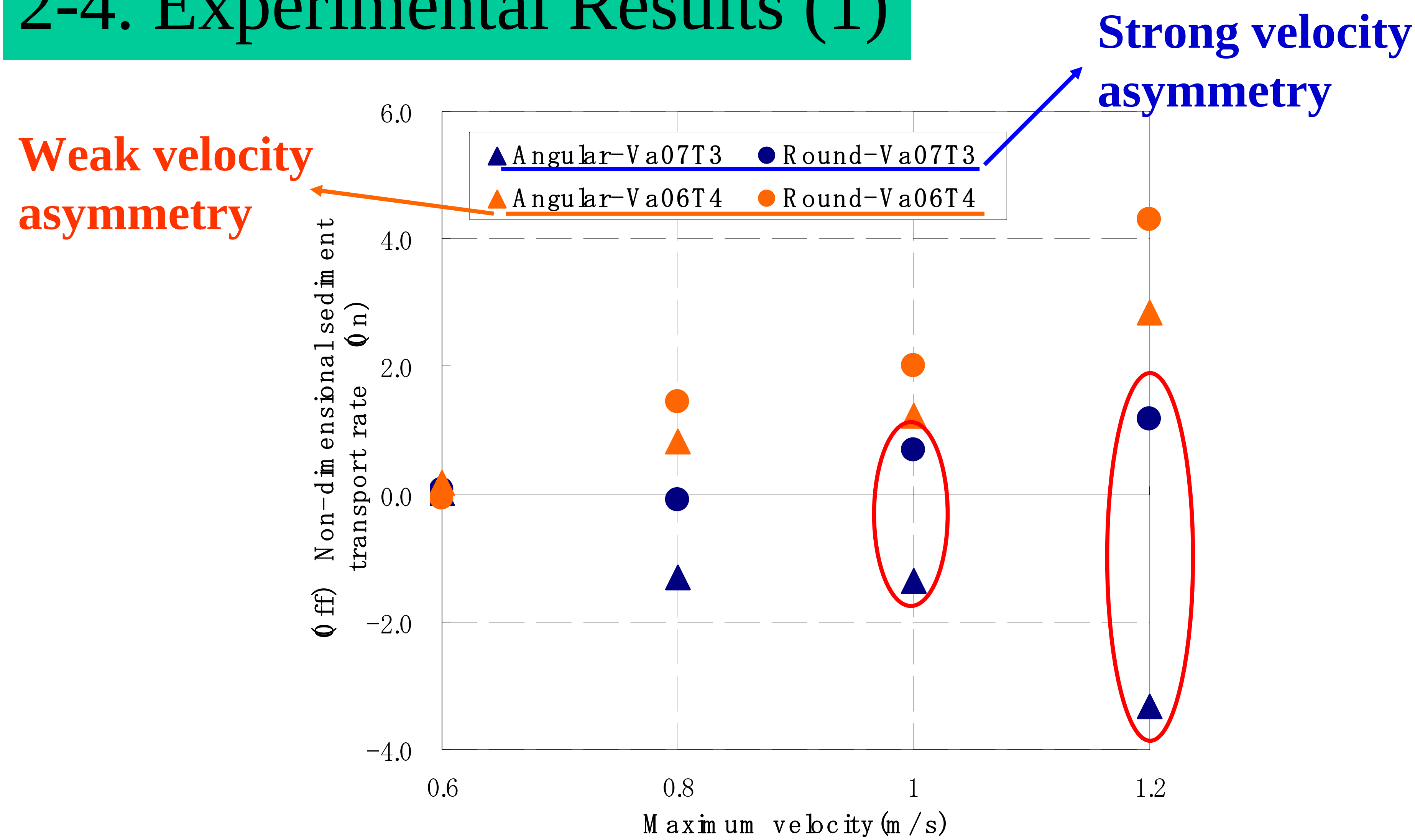

Angular sand: More easily transported to the offshore direction under large velocity and/or strong velocity asymmetry

2-5. Experimental Results (2)

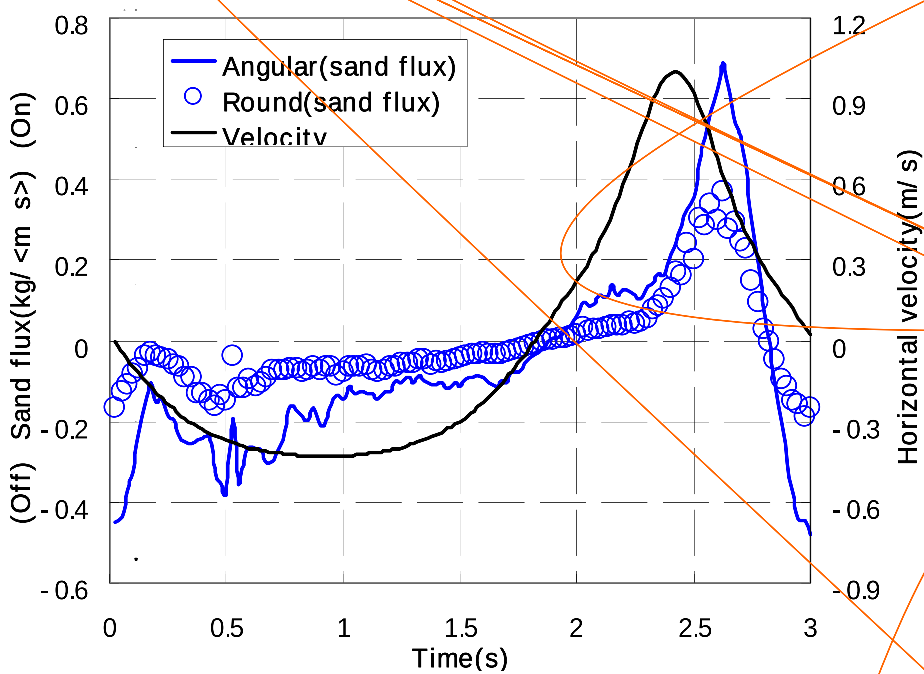

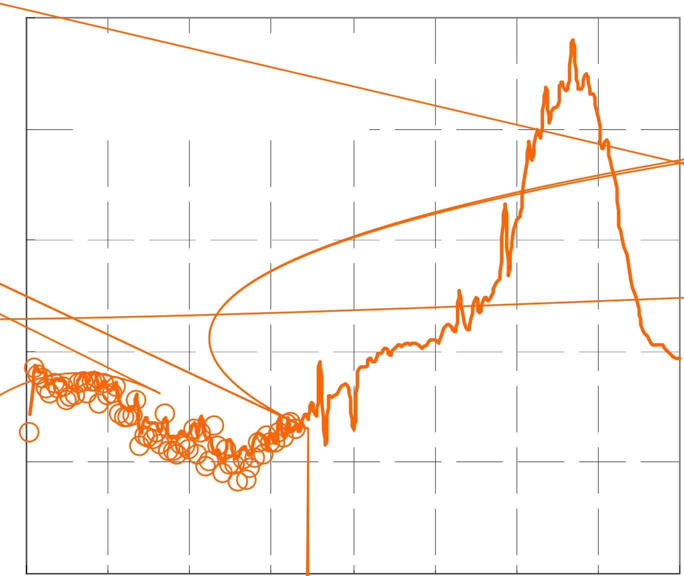

3-1. Two-phase Flow Model (1)

$$\frac{\partial \rho(1-C)}{\partial t} + \frac{\partial \rho(1-C)u_j}{\partial x_j} = \frac{\partial \rho \overline{C'u'_j}}{\partial x_j}$$

・・・**Continuity Eq. for fluid phase**

$$\frac{\partial \rho_s C}{\partial t} + \frac{\partial \rho_s C u_{sj}}{\partial x_j} = \frac{\partial \rho_s \overline{C'u'_{sj}}}{\partial x_j}$$

・・・**Continuity Eq. for sediment phase**

$$\frac{\partial \rho(1-C)u_i}{\partial t} + \frac{\partial \rho(1-C)u_i u_j}{\partial x_j} = -\rho(1-C)g\delta_{i2} - (1-C)\frac{\partial p}{\partial x_i} + \frac{\partial T_{ij}}{\partial x_j} - f_i$$

・・・**Momentum Eq. for fluid phase**

$$\frac{\partial \rho_s C u_{si}}{\partial t} + \frac{\partial \rho_s C u_{si} u_{sj}}{\partial x_j} = -\rho_s C g \delta_{i2} - C\frac{\partial p}{\partial x_i} + \frac{\partial T_{sij}}{\partial x_j} + f_i$$

・・・**Momentum Eq. for sediment phase**

ρ: Density, u: Velocity, C: Sediment concentration, p: Pressure, g: Gravitational acceleration, Tij: Turbulent stress, Tsij: Inter-granular stress, fi: interaction force, Kz: Turbulent diffusivity, ϕ: Dynamic friction angle of sediment <Subscripts> i, j: Horizontal and vertical directions, s: Sediment phase

$$u = U_\infty,\ -Cw_s + K_z\frac{\partial C}{\partial z} = 0$$

・・・**Upper boundary condition**

$$u = u_s = w = w_s = 0$$

・・・**Lower boundary condition**

$$f_x + \frac{\partial T_{sxz}}{\partial z} - C\frac{\partial p}{\partial x} > \frac{C}{C_{\max}}(\rho_s - \rho)gC\tan\phi \Rightarrow u_s = 0$$

・・・**Dynamical bottom condition**

3-2. Two-phase Flow Model (2)

The difference of shapes of sands ⇒ Drag coefficient, fall velocity, dynamic friction angle, C_{max}

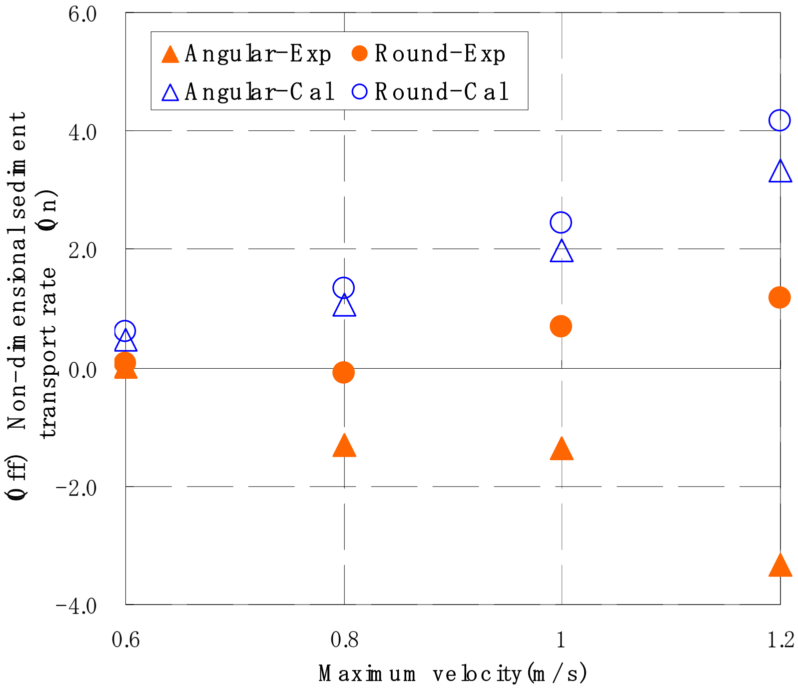

Sediment transport rate

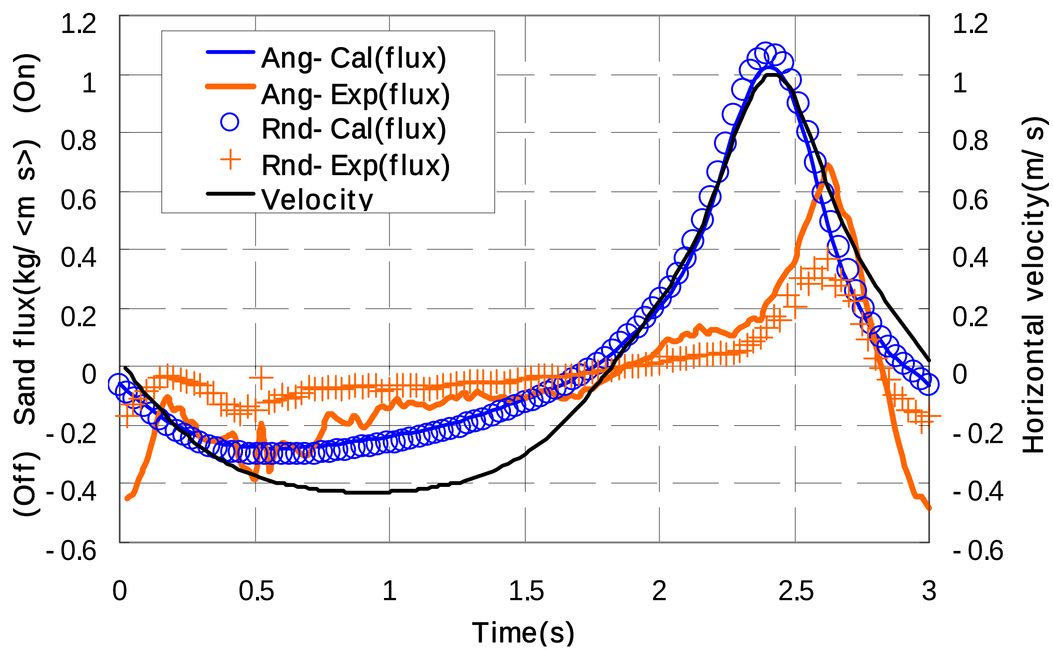

Sand flux

The existing model fails to reflect the effect of shape of sand

3-3. Modeling of Dynamic Pore Water Pressure (1)

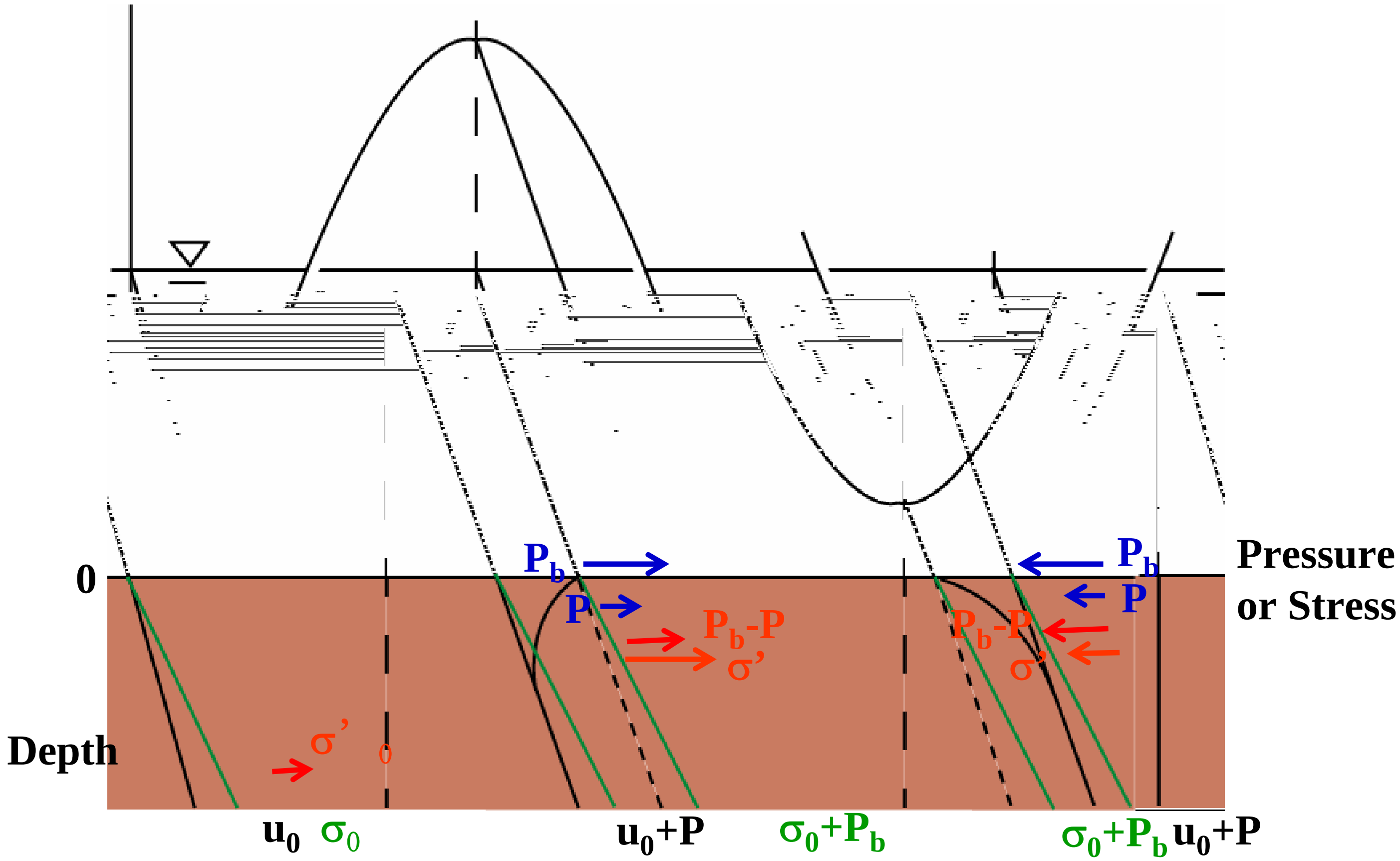

$$\sigma'_0 = \sigma_0 - u_0 \;\Rightarrow\; \sigma' = \underline{(\sigma_0 + p_b)} - \underline{(u_0 + p)} = \sigma'_0 + p_b - p$$

Effective stress | **Total stress** | **Pore water pressure**

Pressure change at the sea bottom (P_b) = Total stress change

Pressure change in the sea bed (P) = Pore water pressure change

3-4. Modeling of Dynamic Pore Water Pressure (2)

◇**Delay and damping of the propagation of water pressure change into the sea bed ⇒ Effective stress change (Dynamic effective stress = P_b - P)**

◇**Differences in k, m_v, S_r, and n ⇒ Different dynamic effective stress**

$$C\frac{\partial^2 p}{\partial z^2} = \alpha\frac{\partial p}{\partial t} - \frac{\partial p_b}{\partial t}$$

$$C = \frac{k}{\gamma_w m_v}, \quad \alpha = 1 + \frac{n}{m_v}\left(\frac{1-S_r}{p_{mg}}\right)$$

Governing eq. for dynamic pore water pressure

	Angular	**Round**
C (m^2/s)	1.699	2.364
α	4.305	3.814

Angular: Less consolidated, more compressible pore volume

k: Permeability, γ_w: Specific weight of water, m_v: Coefficient of volume compressibility, S_r: Saturation ration, n: Porosity, p_{mg}: Absolute value of pore water pressure

3-5. Modeling of Dynamic Pore Water Pressure (3)

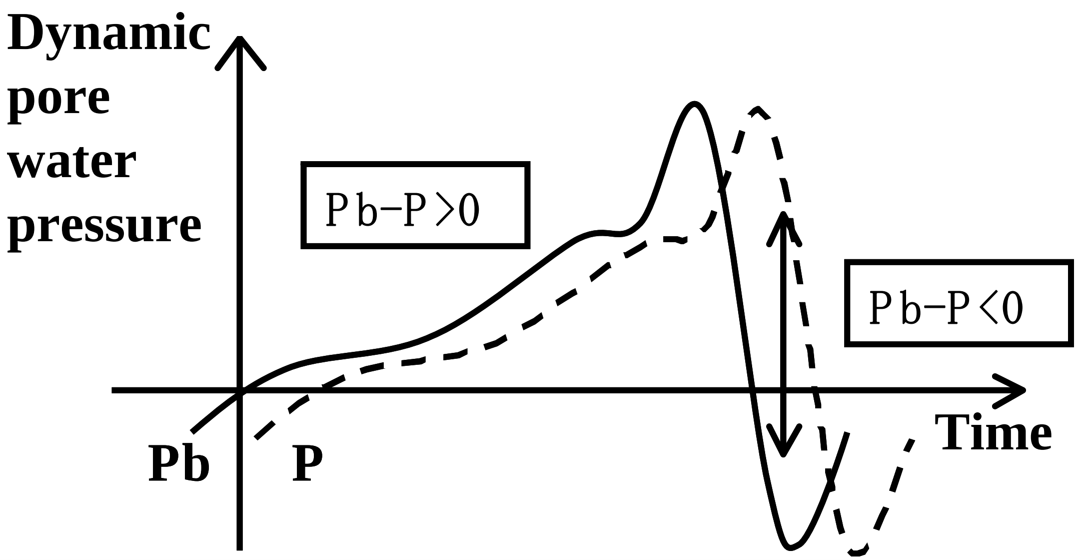

Dynamic water pressure decreases (negative velocity acceleration) ⇒ Negative effective stress

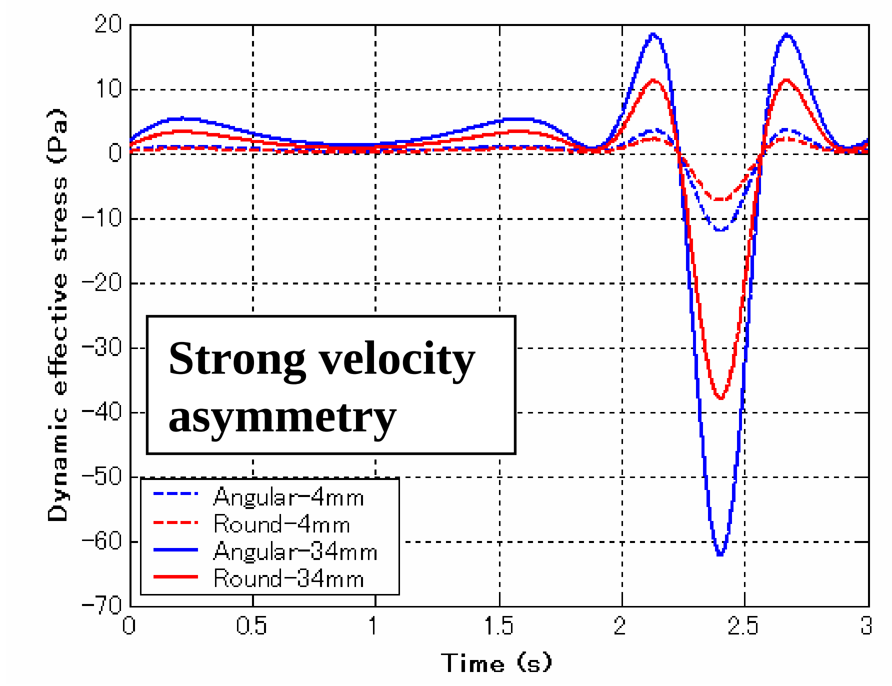

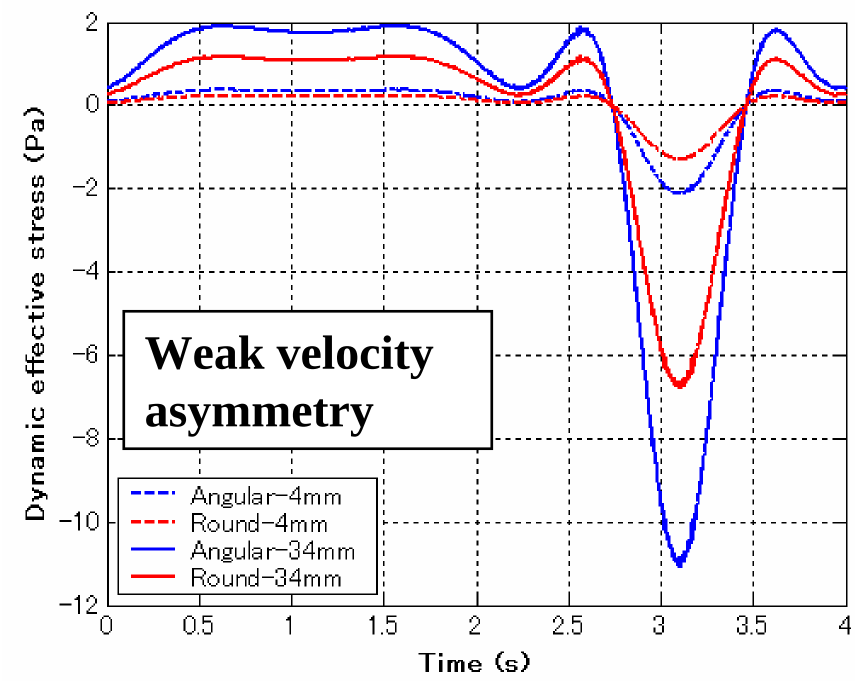

3-6. Modified Two-phase Flow Model (1)

Angular sand (small saturation ratio, more compressible pore volume) under strong velocity asymmetry wave ⇒ Large negative dynamic effective stress

Modification of the two-phase flow model considering dynamic effective stress ($\sigma' = P_b - P$)

$$f_x + \frac{\partial T_{sxz}}{\partial z} - C\frac{\partial p}{\partial x} > \frac{C}{C_{\max}}(\rho_s - \rho)gC\tan\phi \boxed{-\frac{\partial \sigma'}{\partial z}C\tan\phi} \cdots$$

Dynamical bottom condition

Force on sand particles

Frictional resistance of sand particles

3-7. Modified Two-phase Flow Model (2)

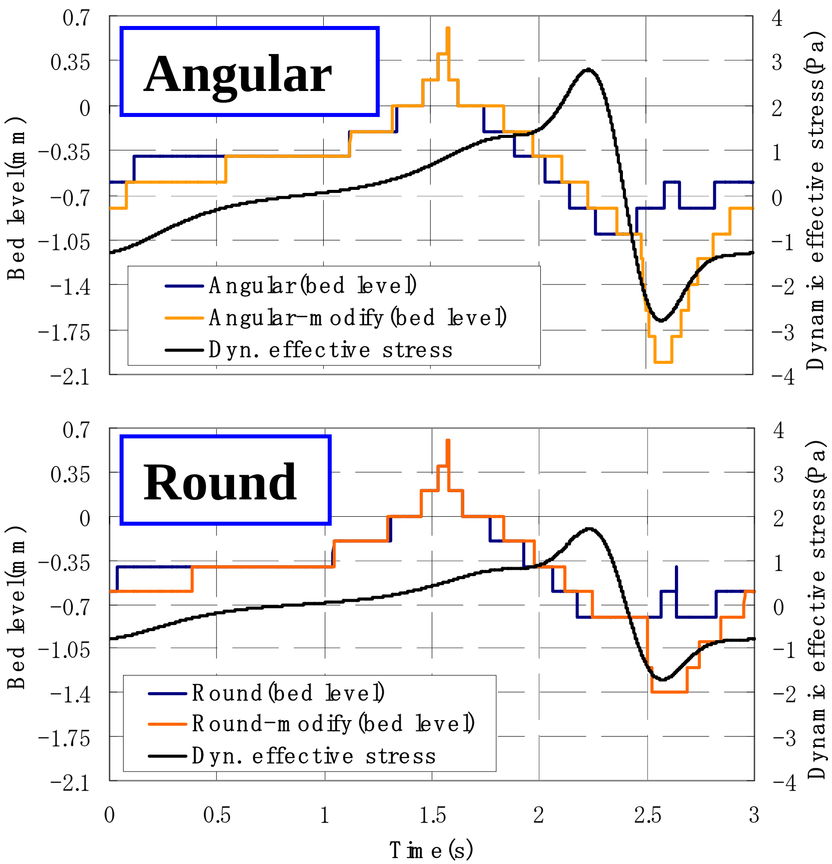

Sea bed level

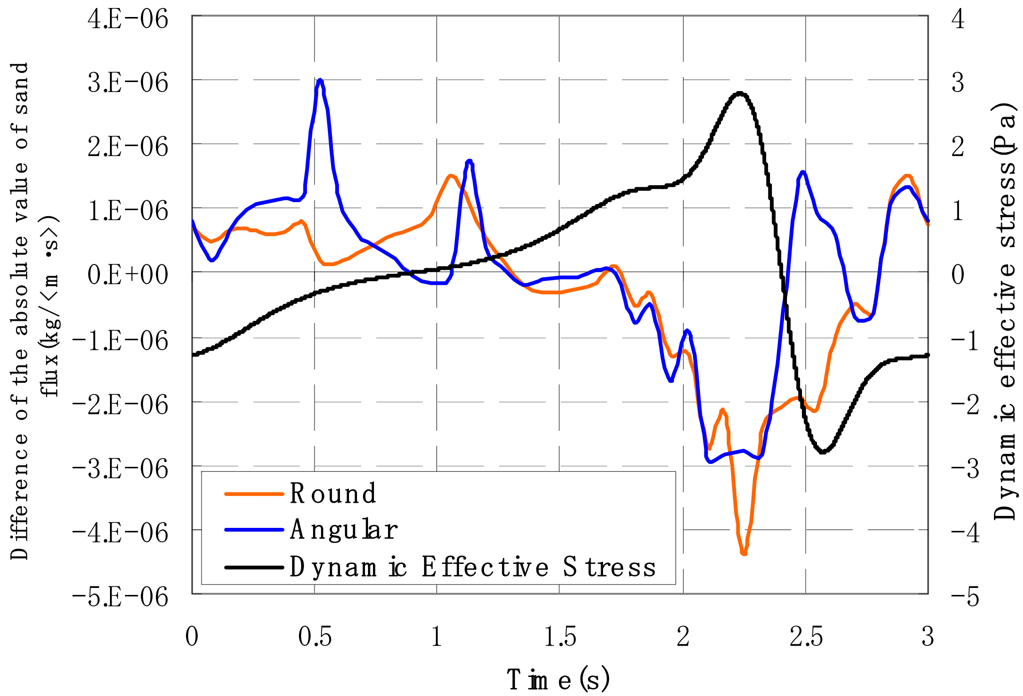

The difference of sand flux between before and after the modification

Considering dynamic effective stress ⇒ Erosion depth

3-8. Modified Two-phase Flow Model (3)

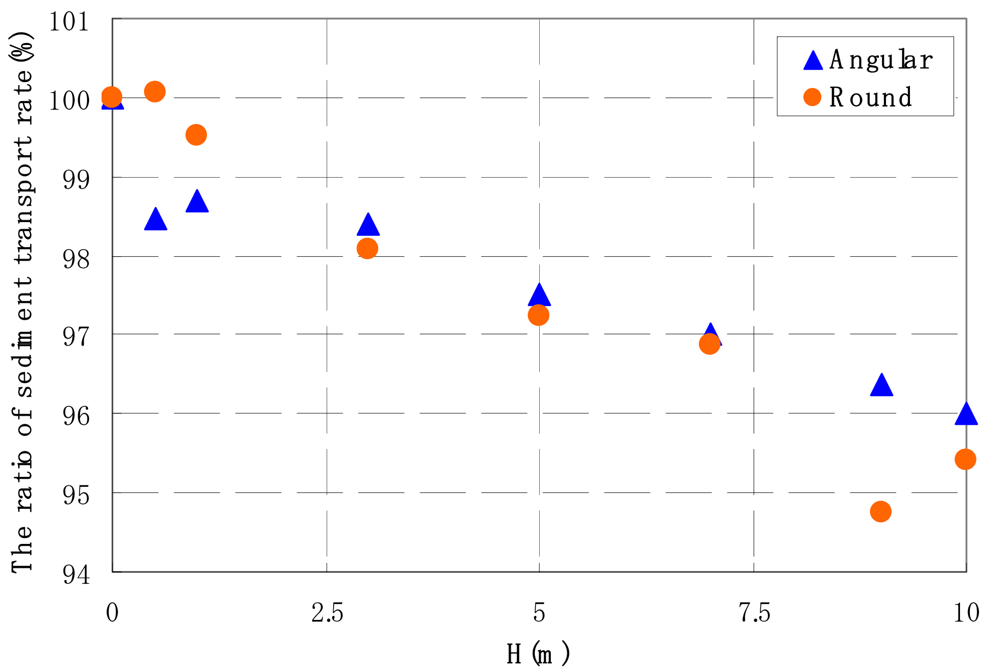

The ratio of sediment transport rate of the modified model to that of the existing model

1. **Dynamic effective stress ⇒ Sediment transport to the offshore direction**

2. **Little difference between angular and round sands and the sediment transport rate to the onshore direction for angular sand ⇒ Left to be challenges**

4. Conclusions

◆**Characteristics of angular sand compared with round sand**

◇**Easily moved and more suspended.**

◇**Suspended sediment during the onshore flow does not fall down completely before the flow reversal ⇒ Sediment transport rate tends to the offshore direction**

◇**Under strong velocity asymmetry wave, because of low saturation ratio larger negative dynamic effective stress develops**

◆**Two-phase flow model considering dynamic effective stress**

◇**Erosion depth and sediment flux increase**

◇**Sediment transport rate changes to the offshore direction (in accordance with the laboratory measurements)**

tsunami inundation

rapid pressure change, flooding over unsaturated bed

1. Introduction

- Severe coastal erosion (1.6 km^2/yr in Japan)

  ⇒ Strong demand for stable beach nourishment
- Various materials for beach nourishment
  - Round shape (sand in natural beach)
  - Angular shape (sand made of crashed rocks)

  ⇒ Little studies on the effect of shapes of sands on sediment transport

Objectives: To identify the effect of shapes of sands on sediment transport by investigating the following 2 points

- Sediment movement mechanisms by laboratory measurements
- Dynamic pore water pressure by numerical computation